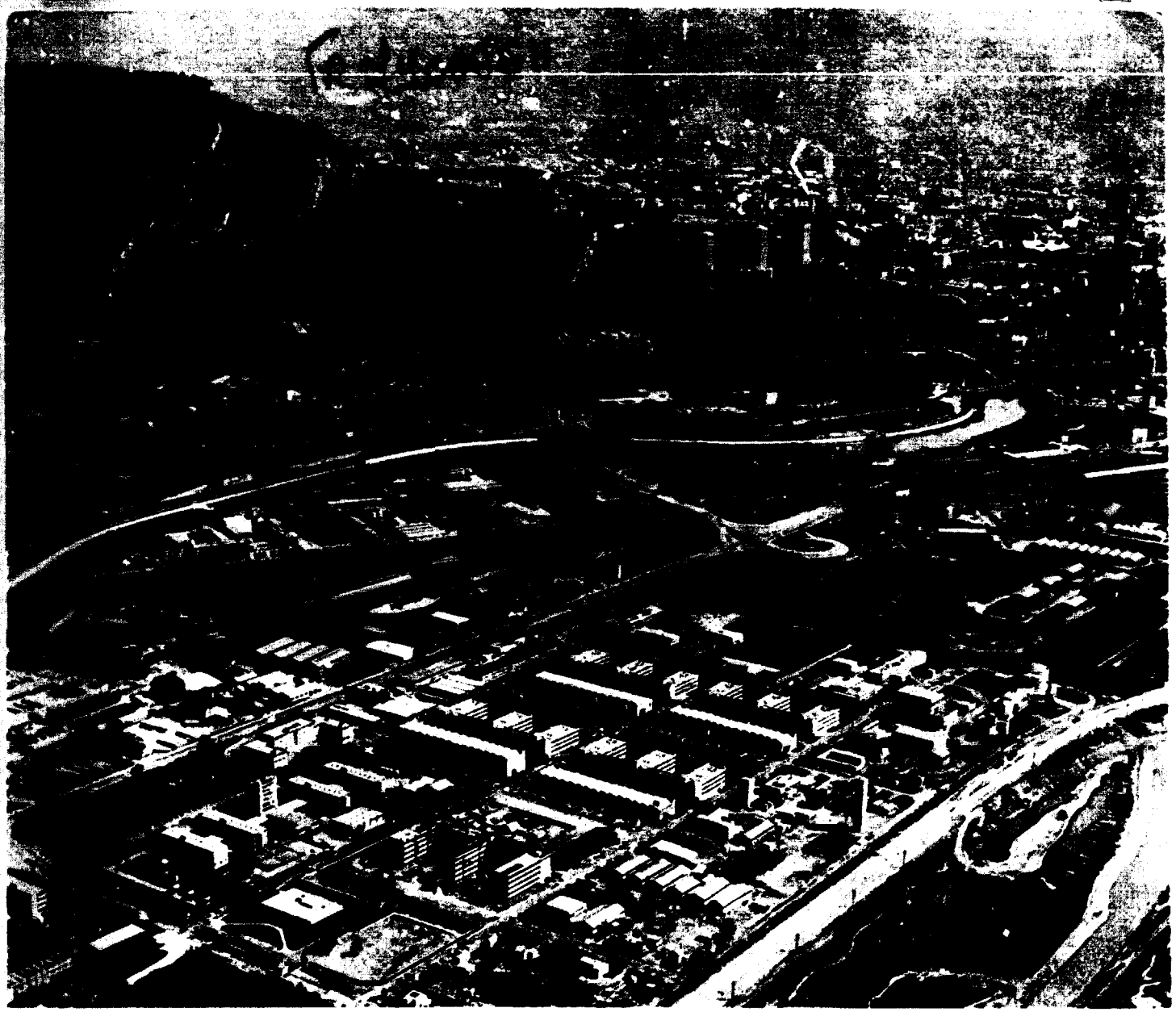

COMMISSARIAT
A L'ENERGIE
ATOMIQUE

LABORATOIRE
D'ELECTRONIQUE
ET DE
TECHNOLOGIE
DE L'INFORMATIQUE

CENTRE D'ÉTUDES NUCLÉAIRES
DE GRENOBLE

C.E.A. - C.E.N-G

LABORATOIRE D'ELECTRONIQUE ET DE
TECHNOLOGIE DE L'INFORMATIQUE

Laboratoire de Microélectronique
Physique

Grenoble le 12 Septembre 1978

International Conference on Ion Beam Modification of Materials. Budapest, Hongrie, 4-9 septembre 1978.
CEA-CONF-4444

HIGH DOSE IMPLANTATIONS OF ANTIMONY FOR BURIED LAYER APPLICATIONS

J.P.GAILLIARD - M. DUPUY - M. GARCIA
J.C. ROUSSIN - M. ROCHE *

* Sescosem. St Egève

RESUME

HIGH DOSE IMPLANTATIONS OF ANTIMONY FOR BURIED LAYER APPLICATIONS

J.P. GAILLIARD - M. DUPUY - M. GARCIA - M. ROCHE

We have studied electrical and physical properties of high dose plantations of antimony in silicon for use in buried layer applications.

The results have been obtained both on <111> and <100> oriented silicon fers. Following implantations which lead to amorphization we perform an annealing 600°C for 10 mn in order to recrystallize the layer. The observed electrical operties (μ, R) show that the concentration of electrically active antimony ions greater than that predicted from the solubility of antimony in silicon. Further nealing (in the range 1050°C - 1200°C) induces : firstly a precipitation of the and secondly a diffusion and dissolution of the precipitates. There is a fferent evolution of the defects in the <111> and <100> silicon slices.

T.E.M. reveals no defects in the <100> wafers after one hour annealing 1200°C, whereas defects and twins remain in <111> wafers.

Having obtained the evolution of R with time and temperature we have en determined the implantation and annealing conditions which lead to the low sistivity (R = 10) needed for buried layer applications. Results with very ny industrialy made devices will be discussed.

HIGH DOSE IMPLANTATIONS OF ANTIMONY FOR BURIED LAYER APPLICATIONS

J.P GAILLIARD, M. DUPUY, M. GARCIA*, J.C. ROUSSIN
LETI-CENG - 85 X - 38041 GRENOBLE - France

M. ROCHE
THOMSON - SESCOSEM - 38120 ST EGREVE - France

Low resistance layers, n type, typically 10 to 20 Ω per square, are of utmost importance in integrated circuit technology. In order to get a high density of integration the extension of the layer must be limited in depth. The layer must also present few defects in order to lead to a covering epitaxial layer of high quality. In addition, the dopant in the low resistance buried layer should not diffuse too freely and contaminate the upper epitaxial film. This last condition leads us to eliminate phosphorus as a doping impurity, and antimony looks to be the most promising impurity although arsenic, up to now, has been extensively used because the predeposition step in a furnace is easier. Ion implantation with the new high current machines allows us to overcome this drawback. This paper presents results concerning the realization of low resistance layers using antimony implantation, the effect of heat treatments on some electrical parameters and the evolution of crystalline defects in these layers. Examples of industrial applications will be given.

I EXPERIMENTAL

With the aim of making low resistance layers, we limit ourselves to doses from 5.10^{14} cm^{-2} up to 10^{16} cm^{-2}. Implantations have been performed with a 200-1000 Extrion high current machine. Silicon p type, 40 Ω-cm of <111> or <100> orientations has been used as a substrate.

After implantation a first annealing, 800° C - 10 mn, has been performed in order to restore the crystallinity of the layer which had been amorphized during implantation. After this annealing stage, resistivity of the layer can be measured using the four point probes

* Now at Motorola - Le Mirail BP 3411 - 31023 TOULOUSE - France

method , and we found, whatever the dose used, 50 Ω <$R_\square$<100 Ω.

Starting from these samples we have made isothermal annealings at 1050°C, 1100°C, 1150°C or 1200°C with time ranging from 10 mn to 50 hours ; after each treatment $R_\square$ and x_j were measured. For an antimony implanted dose of $3.10^{15} cm^{-2}$, the junction depth is plotted in figure 1 as a function of annealing time for different temperatures. In figure 2, we show the annealing curves at 1200°C for different doses, and in figure 3 at $2.10^{15} cm^{-2}$ for different temperatures. For low temperatures, for example at 1050°C (fig. 3) we remark that a reverse annealing stage is clearly visible.

II INTERPRETATION

The interpretation of the results is presented in term of antimony precipitation in the implanted layer, TEM studies will support this interpretation.

After the initial heat treatment (800°C - 10 mn) the amorphous layer has been recrystallized but the duration was not sufficient to allow the supersaturated antimony to precipitate : limit of solubility is about $2.10^{19} cm^{-3}$ for antimony in silicon to be compared with $5.10^{20} cm^{-3}$ antimony in the implanted layer.

The resistance of 50 Ω per square mentionned previously can be explained only if we suppose that the supersaturated impurity is largly electrically active [1]. When annealing at hight temperature takes place, antimony precipitates and the resistance of the layer is increased. The precipitation needs a relatively long time t_p to occur, which, for $2.10^{15} cm^{-2}$ can be evaluated as follow :

T° C	1050	1100	1150	1200
t_p mn	≈ 60	≈ 40	≈ 25	<10

For longer annealing times diffusion takes place and the layer can be interpreted as a constant concentration source of antimony, with $C_s = 2.10^{19} cm^{-3}$ equal to the limit of solubility. After a time t,

the quantity of impurity which has diffused into the silicon is :

$$Q(t) = \frac{2 C_s}{\sqrt{\pi}} \sqrt{Dt}$$

where D is the diffusivity of antimony in silicon at the annealing temperature. If Q (t) is electrically active, we have :

$$Q(t) = \frac{1}{R_\square q \mu}$$

So, if we plot $\frac{1}{R_\square}$ versus $\sqrt{t}$, we should obtain a straight line. Experimental results (fig 4) support this interpretation, and a detailed analysis of the data gives, for the diffusivity at 1200°C a value of :

$$D_{1200} = 2.10^{-12} cm^2 s^{-1}$$

with $\mu = 100\ cm^2\ V^{-1}\ s^{-1}$ and $C_s = 2.10^{19} cm^{-3}$.

This D value, higher than the tabulated ones [2] [3] , should be valid at a concentration near the solubility limit. Figure 4 shows that, at 1200°C the line bent and $\frac{1}{R_\square}$ becomes saturated indicating that all the precipitates have been dissolved. The interpretation we propose looks coherent, and we have confirmed its validity by studies of the layers by transmission electron microscopy.

III TRANSMISSION ELECTRON MICROSCOPY

Thin foils (less than 1 µm) are obtained by chemical polishing from the back side. Specimens are observed in a 200 keV microscope equipped with a tilting specimen holder. Stereomicrographs are obtained in order to study the three dimentional dislocation arrangements. Results are presented for <100> and <111> substrate orientations.

- <100> orientation :

After the first annealing (800°C - 10 mn), the implanted layer exhibits a high density of small defects (less than 500 Å) identified as dislocation loops. Diffraction patterns obtained from various orientations by tilting, show no extra spots coming from either antimony precipitation or twins.

Figure 5 (a) is typical of a specimen implanted at $2.10^{15} cm^{-2}$ and annealed at 1050° C for 10 mn. Three kinds of dislocation loops are present : Frank loops (arrowed A, Burgers vectors $\frac{1}{3}$ <111>), perfect loops (arrowed B, Burgers vectors $\frac{1}{2}$ <110>, situated in inclined {110} planes, and eventually large loops laying in the (100) plane parallel to the surface. The corresponding diffraction pattern exhibits rings due to the presence of fine antimony precipitates (~100 Å in diameter).

As the annealing goes on, three phenomena are observed. First of all, the size and density of the loops A and B are decreased. These loops finally disappear after approximatly 30 mn. Secondly, the loops C grow up and reach a critical size of approximatly 1 µm allowing an interaction and a reorganization of these defects. Thirdly, the antimony precipitation becomes more important. After a 60 mn annealing time (figure 5 (b)), it can be noticed that A and B defects are not present any more. The interaction of C defects leads to the formation of a dislocation network. Antimony precipitations are clearly visible on this picture. For longer annealing times, diffusion of antimony induces the dissolution of precipitates. The dislocation network itself reaches the surface by gliding and vanishes. As an example, a 1200° C - 5 hours annealing, leads to a layer free from crystalline defects (implanted dose : 2.10^{15} cm^{-2}).

- <111> orientation :

After the first annealing (800°C - 10 mn) the implanted layer presents a great density of dislocation loops. But, in addition, numerous micro-twins are detected. They are generated during the recrystallization of the amorphous layer. It is thought that these micro-twins, which are very stable, play an important role towards

the annealing of defects. It is a matter of fact that these twins inhibit the gliding of dislocations thus preventing them from reaching the surface to annihilate. Figure 5 (c) shows islands of defects after a 1050° C - 10 mn annealing. These tangles of defects remain even after a longer time annealing of 1200° C - 60 mn (fig 5 d) where micro-twins are still present. As far as antimony precipitation is concerned no significative difference is noticed between <100> and <111> silicon.

This TEM study points out that residual defects are much more difficult to eliminate if <111> silicon orientation is used compared to <100>. If one considers that the realization of an epitaxial layer is easier for a <100> orientation and takes place at a lower temperature than for <111> , it is rather surprising to notice that all the devices are traditionally realized on <111> wafers.

IV APPLICATIONS

The principal features of antimony implantation being understood, we proceed to the realization of devices with an antimony buried layer. To determine the conditions of implantation and annealing we use the diagram presented in fig 6. Choosing the desired $R_{\square}$ and x_j leads to a dose and an annealing temperature. The second quadrant gives us the necessary time of heat treatment ; and the third quadrant shows us if this time is sufficient in order to get a precipitate free layer. This is not the case for point J, but this is the case for point K which was choosen at such a high temperature in order not to modify the traditionnal diffusion temperature used at Thomson in the fabrication of the operational amplifier SFC 2776. Antimony buried layer have also been used for the LF 155 operational amplifier with J.FET input. Finally audio 20 W amplifiers have also been processed in this case antimony dose was as high as 5.10^{15} cm^{-2} to get $R_{\square} = 10\ \Omega$. The main results obtained with these devices are a high reproducibility and homogeneity of the low resistance layer and a good quality of the epitaxial layer grown upon it.

V CONCLUSION

In this paper we have shown the principal features of high doses antimony implantation, and we have given a simple explanation in term of antimony precipitation. TEM studies support this explanation and show futhermore, that <100> orientation presents less defects than <111>. Finally introduction of antimony predeposition by ion implantation in the industrial process of devices fabrication leads to a good reproducibility and increases the yields.

BIBLIOGRAPHY :

1 M.D. MATTHEWS
J. Mat. Scien. 4. 997 (1969)

2 J.J. ROHAN - N.E. PICKERING - J. KENNEDY
J. Elec. Soc. 106. 705 (1959)

3 C.S. FULLER - J.A. DITZENBERGER
J. Appl. Phys. 27. 554 (1956)

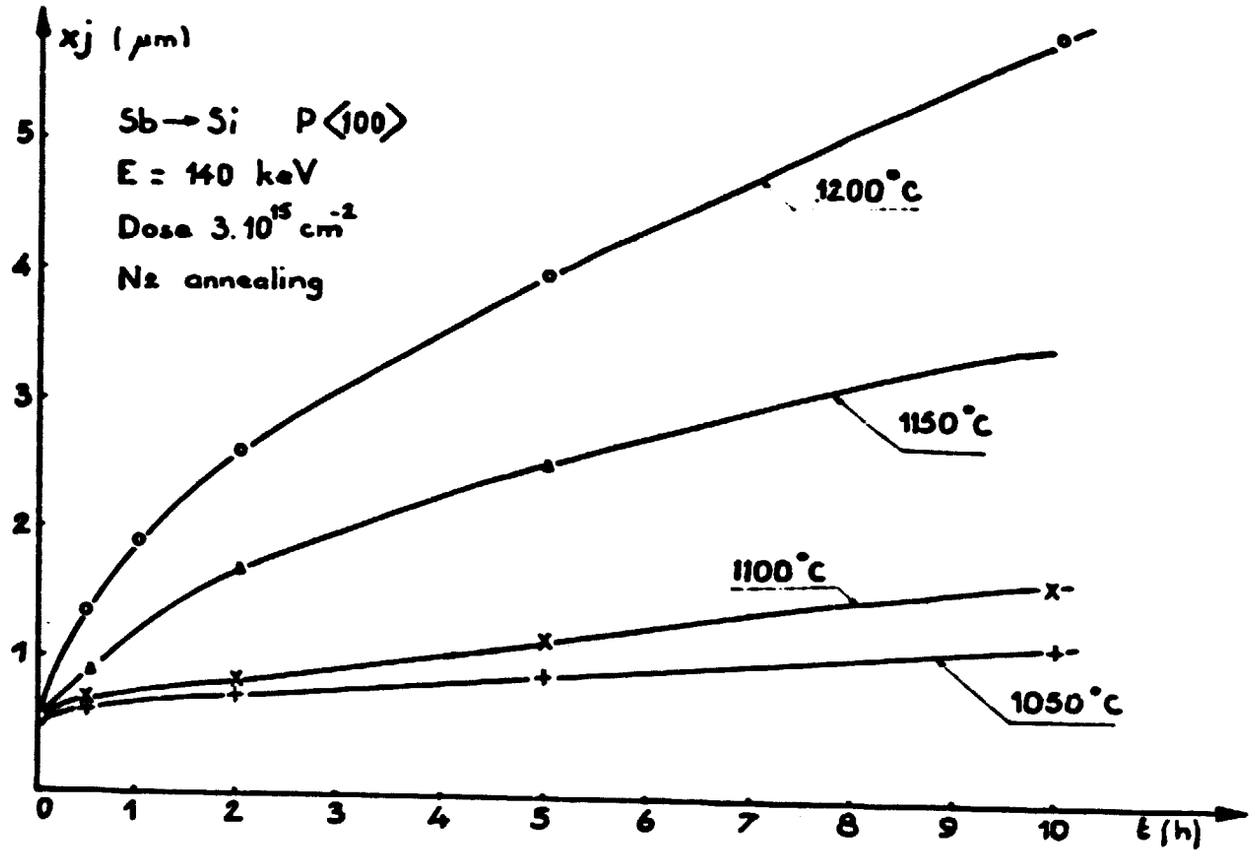
xj (μm)
Sb → Si P ⟨100⟩
E = 140 keV
Dose 3.10^15 cm^-2
N2 annealing
1200°C
1150°C
1100°C
1050°C
0 1 2 3 4 5 6 7 8 9 10 t (h)

fig 1

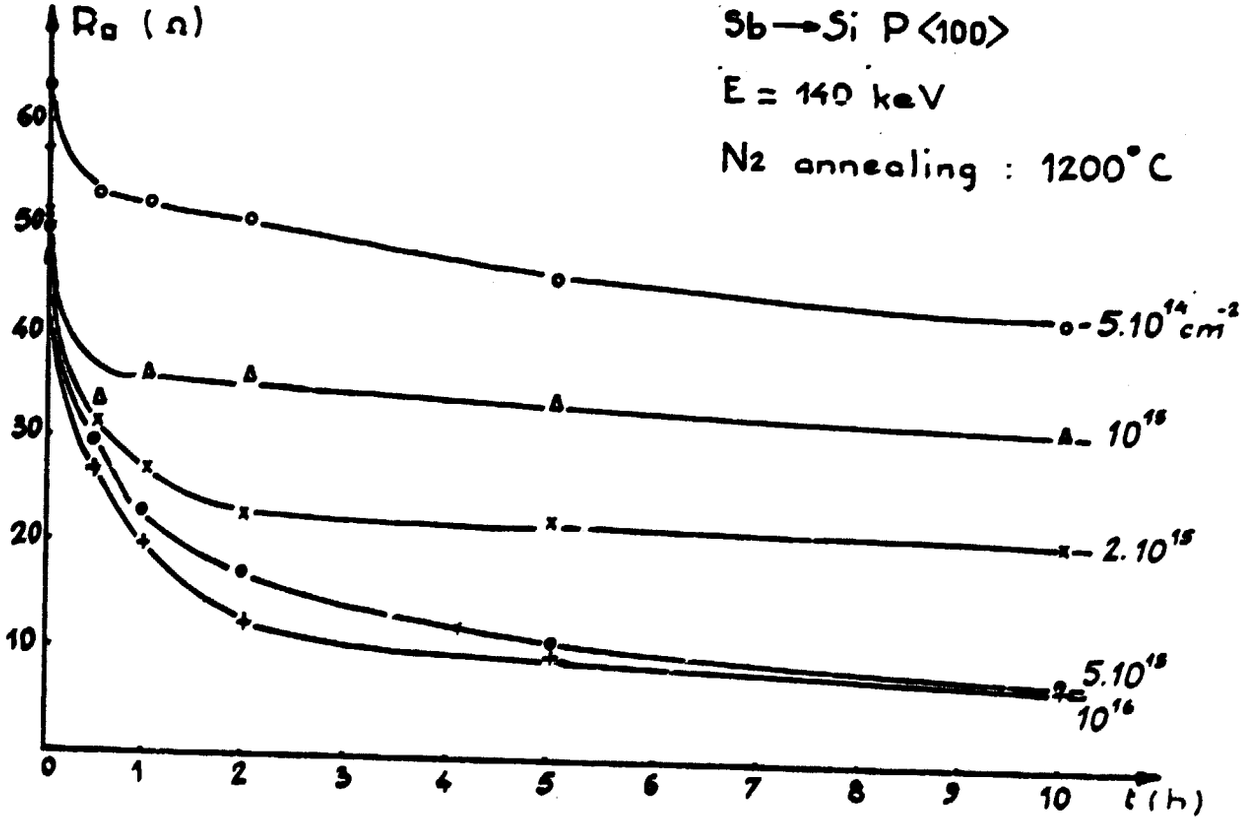
Rs (Ω)
Sb → Si P ⟨100⟩
E = 140 keV
N2 annealing : 1200°C
5.10^14 cm^-2
10^15
2.10^15
5.10^15
10^16
0 1 2 3 4 5 6 7 8 9 10 t (h)

fig 2

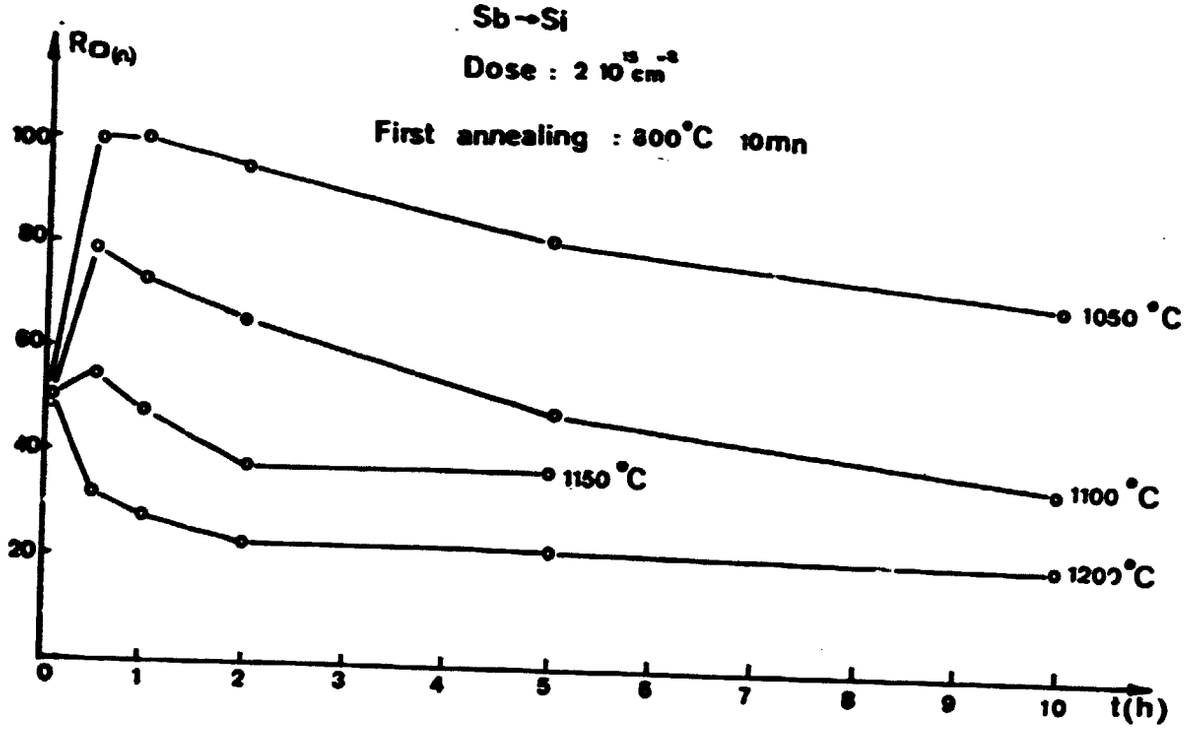
Sb→Si
Dose : 2 10^15 cm^-2
First annealing : 800°C 10mn
R□(Ω)
100
80
60
40
20
0
1
2
3
4
5
6
7
8
9
10
t(h)
1050 °C
1100 °C
1150 °C
1200°C

fig 3

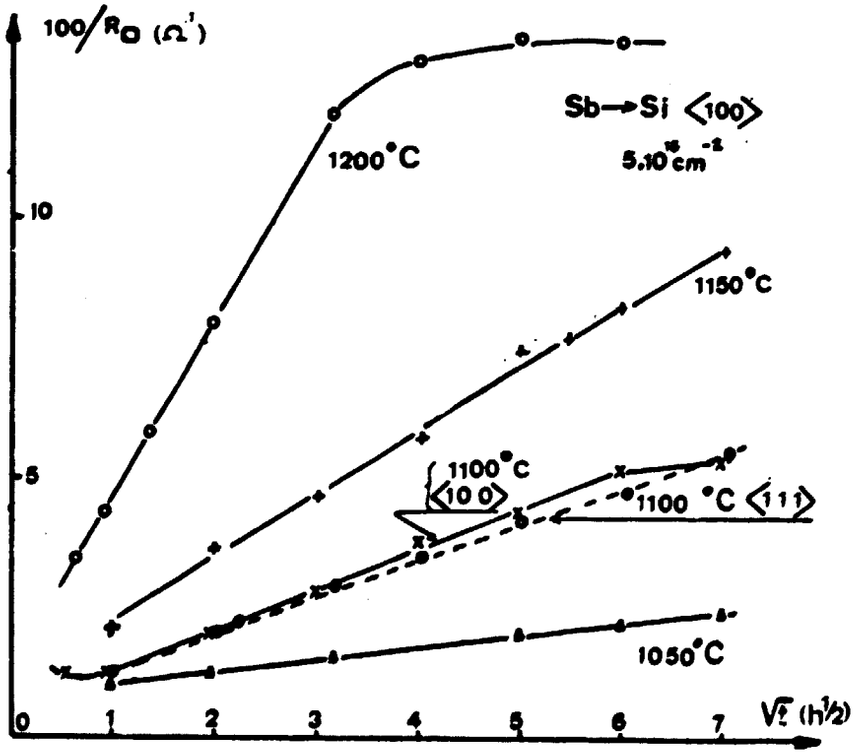
100/R□ (Ω⁻¹)
Sb→Si ⟨100⟩
5.10^15 cm^-2
1200°C
10
5
1150°C
1100°C
⟨100⟩
1100 °C ⟨111⟩
1050°C
0
1
2
3
4
5
6
7
√t (h^1/2)

fig 4

Sb Implanted dose $2\ 10^{15}\ cm^{-2}$

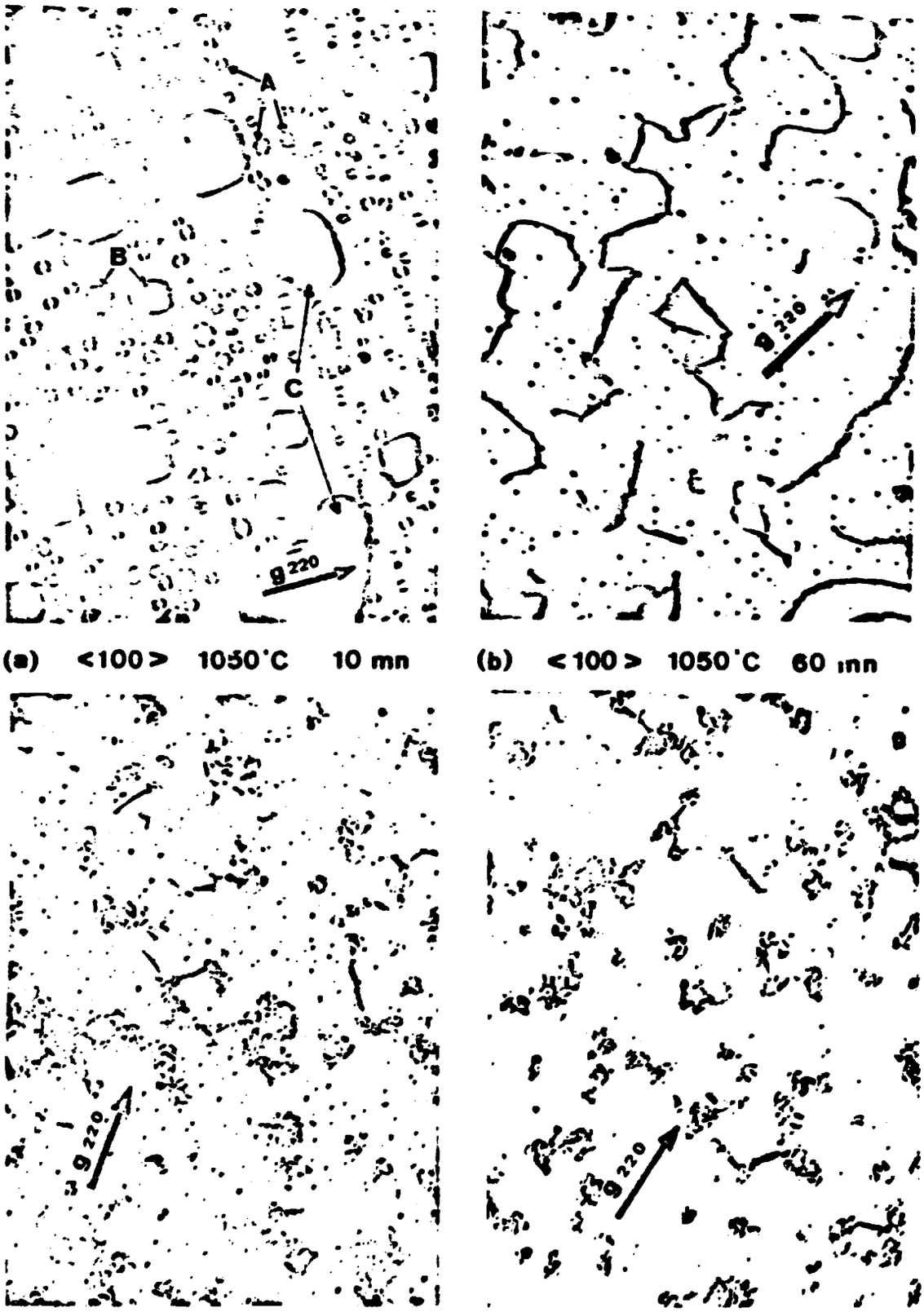

(a) <100> 1050°C 10 mn

(b) <100> 1050°C 60 mn

(c) <111> 1050°C 10 mn

(d) <111> 1200°C 60 mn

1 µm

fig 5

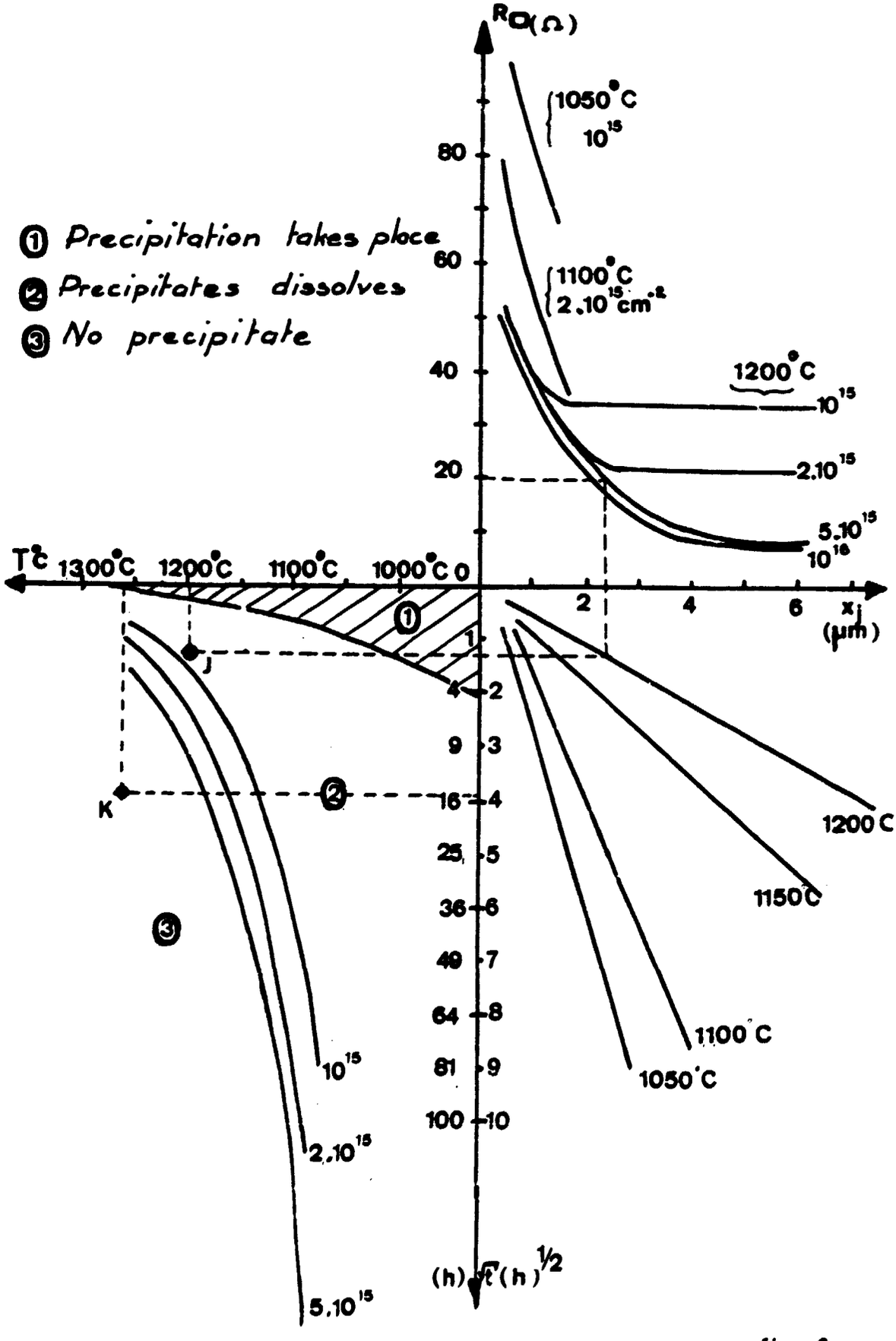
① Precipitation takes place
② Precipitates dissolves
③ No precipitate
$R_\square(\Omega)$
1050°C
10^{15}
1100°C
$2.10^{15}\,cm^{-2}$
1200°C
10^{15}
2.10^{15}
5.10^{15}
10^{16}
80
60
40
20
0
T°C
1300°C
1200°C
1100°C
1000°C
2
4
6
x_j (µm)
J
K
1
2
3
4
5
6
7
8
9
10
1
4
9
16
25
36
49
64
81
100
1200°C
1150°C
1100°C
1050°C
10^{15}
2.10^{15}
5.10^{15}
(h) $\sqrt{t}$ $(h)^{1/2}$

fig 6